NanoNEXT

Research Article

DOI: 10.54392/nnxt2431

Nanocomposite 2D Graphene Synthesized Various TMDs (MoS_2, CoS_2 and NiS_2) as a Counter Electrode for Platinum Free Efficient Dye-Sensitized Solar Cells

J. Dineshkumar [a], R. Sakthivel [b,*], A. Geetha [c]

[a] Department of Electronics, RVS College of Arts & Science, Sulur, Coimbatore-641402, Tamil Nadu, India.
[b] Department of Electronics, PSG College of Arts & Science, Civil Aerodrome Post, Coimbatore-641014, Tamil Nadu, India.
[c] Department of Chemistry, Hindustan College of Arts & Science, Hindustan Gardens (Behind Nava India), Avinashi Road, Coimbatore- 641028, Tamil Nadu, India.
* Corresponding author Email: rsgvel@gmail.com
DOI: https://doi.org/10.54392/nnxt2431
Received: 05-07-2024; Revised: 24-08-2024; Accepted: 08-09-2024; Published: 18-09-2024

Abstract: The counter electrode plays a vital role in solarcell performance. Instead of using platinum (Pt) CE, many inorganic and organic counter electrodes (CEs) have been created for dye-sensitized solar cells (DSSCs). However, because of their exceptional chemical stability, low cost, simple fabrication, flexibility, transparence, potential for high efficiency and better electrochemical qualities, carbon nanocomposite and MoS_2 have been crucial to CEs. In this work, we created a graphene nanocomposite with TMDs (MoS_2, CoS_2, and NiS_2) integrated as a counter electrode that can be easily manufactured hydrothermally and utilized in DSSCs. Through the use of energy dispersive spectrum analysis, Raman, scanning electron microscopy, transmission electron microscopy, and X-ray diffraction, the structural, morphological, and elemental content of the samples were examined. In comparison to MoS_2@graphene and CoS_2@graphene, respectively, NiS_2@graphene hybrid demonstrated superior electrical conductivity and catalytic activity as a substitute for platinum counter electrodes in dye-sensitized solar cells (DSSCs). When compared to MoS_2@graphene (7.71 ± 0.03%) and CoS_2@graphene (8.01 ± 0.05%), the resultant NiS_2@graphene counter electrodes (CEs) showed greater power conversion efficiencies (8.42 ± 0.05%). The availability of catalytic edge sites, the three-dimensional (3D) structure of NiS_2, which promotes electrolyte/reactant transport, and the exceptional electrical connection to the underneath graphene are responsible for the exceptional performance of DSSCs. Therefore, our findings show that more research should be done 2D Graphene on the TMDs materials for dye-sensitized solar cells.

Keywords: Graphene, TMDs, Counter Electrode, Dye Sensitized Solar Cells

1. Introduction

In compared to conventional silicon solar cells, dye-sensitized solar cells (DSSCs) have attracted a lot of interest as a potential source of clean energy because of their low cost and relatively high conversion efficiency [1, 2]. The maximum power conversion efficiency (PCE) of 12.3% was recently attained by Yella *et al.* [3] at AM1.5G (100 $mWcm^{-2}$).The working electrode is typically a dye-sensitized TiO_2 nanocrystalline film; the CE is typically a platinized favorable glass; and the electrolyte typically contains an iodide/triiodide (I^-/I_3^-) redox couple between the two electrodes. The sensitizer is photoexcited as part of the working process, and then the semiconductor's conduction band is quickly injected with electrons. After the oxidized dye is regenerated by I in the electrolyte, the resultant I_3^- is reduced to I^- at the CE user experience [4, 5]. CE, a crucial component, plays a crucial role in the performance of DSSC by satisfying electron transport from the CE contact to the electrolyte by electrocatalyzing the reduction of I_3^-. Pt's remarkable chemical stability and electrocatalytic activity in reducing triiodide have made it the material of choice for the CE of DSSCs. However, mass production of DSSCs is hampered by the availability of Pt, a noble metal. Therefore, finding cheaper and more abundant elements to replace Pt is a significant area of research for DSSCs. Carbonaceous compounds [6, 7] and conductive polymers [7] are two examples of materials that have been proposed as CEs to replace Pt in DSSCs. Recently, electrocatalysts made from inorganic materials with high catalytic activity for the reduction of I_3^- have been introduced into DSSCs.

Some examples of these elements include nitrides [8], carbides [9], sulfides [10], oxides [11], and selenides [12].

Effective electrocatalysts for the I_3^-/I^- redox pair in DSSCs include 2D MoS_2, which may also be coupled with G. The G component of these G andMoS_2 composites was first synthesized by adapting the Hummer's method for synthesizing graphene oxide. When compared to the laborious process of chemically connecting individual MoS_2 species to the G surface for decoration, this approach wins out due to the abundance of oxygen-containing functional groups it generates. Nickel sulfides, which have variable atomic ratios depending on the synthesis circumstances, offer significant potential as the CE of DSSCs due to their low cost and high electrocatalytic activity for reducing triiodide. Similar to the reported findings [13], 6–7% PCE was generated using nickel sulfide (Ni_3S_2, NiS) as the CE. Low charge mobility in nickel sulfide nanoparticles, induced by the random boundaries between particles, may, nevertheless, restrict the electrocatalytic activity and, by extension, the performance of solar cells. One possible solution to this problem is a mixture of nickel sulfide and a highly conductive material. It is expected that this composite will serve as a high-performance CE for low-cost DSSCs. Graphene, a two-dimensional carbon material, has recently been proved to be an appropriate photoelectric material [14-17] due to its charge transfer interactions and ballistic conduction of charge carriers. Here, we show how to make nanocomposites TMDs out of graphene nanosheets coated with MoS_2, NiS_2, and CoS_2 in a single, straightforward procedure. This is the first study of TMDs@graphene nanocomposites specifically for DSSCs to the best of our knowledge. Graphene has far lower electrocatalytic activity than NiS_2, yet the nanocomposites of NiS_2@graphene show much higher catalytic activity than NiS_2 alone as a result of their synergistic catalysis. NiS_2@graphene CE cells generate 8.42 ± 0.05% PCE, which is much higher than the PCE produced by MoS2@graphene CE cells (7.71 ± 0.03%) and CoS_2@graphene CE cells (8.01 ± 0.05%).

2. Experimental

2.1. Materials

Graphite powders, Sodium molybdate ($Na_2MoO_4.2H_2O$), Nickel nitrate ($NiNO_3.6H_2O$), Cobalt nitrate (($CoNO_3.6H_2O$), and thiourea were bought from Sigma-Aldrich (USA, purity 99.99%). The chemical were used for without supplementary distillation.

2.2. Synthesis of pristine MoS_2@graphene, NiS_2@graphene and CoS_2@graphene based hybrid nanocomposites

The following procedures are used to generate MoS_2 and MoS_2/graphene based hybrid nanocomposites: First, 1 mmol of $Na_2MoO_4.2H_2O$ is dissolved in 4 mmol of thiourea using a magnetic stirrer and a strapping mixture of 60 ml of DI water. After producing GO, we employed the aforementioned solution to disperse the material (0.2 and 0.04 g). After carefully integrating all of the materials, they were enclosed in a Teflon-lined autoclave and heated to 180 degrees Celsius for 24 hours. After the hydrothermal treatment, the product spent 24 hours in a vacuum oven at 80 degrees Celsius to be dried and cleaned. The same process was used to create NiS_2@graphene and CoS_2@graphene composites from Ni and Co sources, respectively.

2.3. Characterization

The structure and morphology of the individual samples were characterized by powder X-ray diffraction (XRD, RigakuDmax/Ultima IV), field emission scanning electron microscopy with EDX facility (FE-SEM, JSM-7600F, JEOL), X-ray photoelectron spectroscopy (XPS, Theta Probe, Thermo Fisher Scientific) and Raman spectroscopy (NRS-3100, JASCO).

2.4. Fabrication of the DSSC

Between the ruthenium-based N719 dye-sensitized TiO_2 film (photoanode) and the TMDs@graphene CE, the I^-/I_3^- redox electrolyte (consisting of 0.05M I2, 0.1M LiI, and 0.1M $LiClO_4$ and dissolved in anhydrous acetonitrile) was injected during DSSC fabrication. A TiO_2 ultrathin layer and a nanocrystalline TiO_2 mesoporous layer of 10 nm thickness were deposited on an FTO substrate, treated with 0.05 M TiCl4 aqueous solution at 90 °C for 30 minutes, and then fused at 450 °C for 30 minutes to prepare the photoanode. The anode was ready after being submerged in a 0.3 mM N719 ethanol solution for 24 hours. Under the irradiation of 100 $mW•cm^{-2}$ of simulated solar light, photocurrent density-voltage (J-V) curves were measured using a solar light simulation. Throughout photovoltaic testing, the mask's aperture size was 22 mm × 22 mm, while the active device area was 20 mm × 20 mm. Before taking any readings, a reference Si cell from NREL was used to calibrate the light intensity. The repeatability and reliability of the

device built with the improved CE material was evaluated by testing up to ten devices.

3. Results and Discussion

3.1. XRD analysis

X-ray diffraction (XRD) spectra are shown in Figure 1 for the identification of the structural characteristics of graphene, MoS_2, and MoS_2/G sheets. The (002) plane of graphene is responsible for the peak at 26.97°, which translates to a d-spacing of 0.38 nm [18]. There is excellent agreement between the standard data (JCPDS card no. 37-1492) and the reflected planes of (002), (100), (103), (105) and (110) from MoS_2. Graphene's (002) plane is present in the MoS_2/G composite, as are all planes linked to MoS_2. Cubic pyrite NiS_2 with lattice parameters of a = 5.67 Å is clearly indexed by the diffraction peaks at 26.8, 31.3, 36.5, 38.1, 45.3, 49.1, 52.3, 53.4, 58.5, 61.2, and 67.0 degrees, which correspond to their characteristic (111), (200), (211), (220), (221), (311), (023), (321), and (400) planes, respectively [19]. The existence of (002) plane coupled with NiS_2 diffraction in the combined samples suggest that nanocomposite were produced among NiS_2 and graphene. the as-synthesized CoS_2/G, which may be classified based on the cattierite CoS_2 phase (JCPDS card 41-1471) at the (200), (210), (211), (220) and (311) diffraction planes, demonstrating the production of the CoS_2 crystalline phase. In addition, the XRD patterns of as-synthesized CoS2/G showed diffraction reflections at 2 of around 26, 8o, which may be attributable to the existence of a graphene phase at the (002).

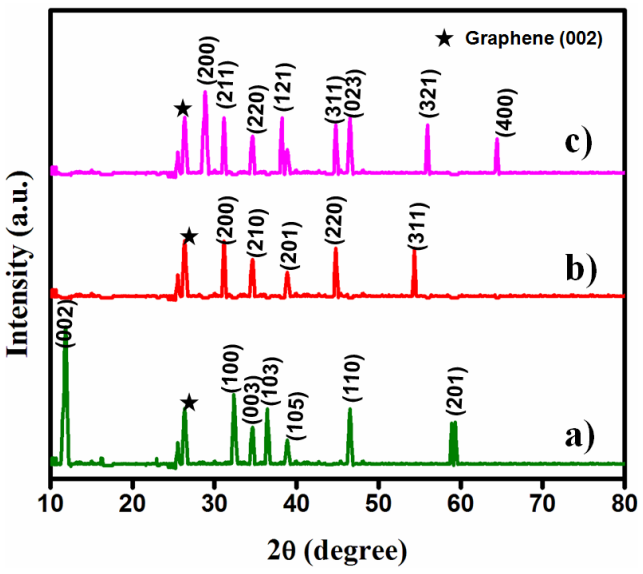

Figure 1. XRD pattern of **(a)** MoS_2@graphene; **(b)** NiS_2@graphene; **(c)** CoS_2@graphene

3.2. Morphological Analysis

The morphological properties of the synthesized samples were analyzed using scanning electron microscopy and transmission electron microscopy. Figure 2 displays SEM images of composite samples made of MoS_2@graphene (a), NiS_2@graphene (b), and CoS_2@graphene (c). Graphene has a 2D sheet form with a wrinkled surface. The nanoparticles used in the MoS2, NiS2, and CoS_2 experiments were all round and had sizes between 30 and 40 nm; they were uniformly placed on the surface of the graphene nanosheets. Additional transmission electron microscopy (TEM) images of MoS_2@graphene (Figure 2d) and NiS_2@graphene (Figure 2e) validated the SEM results and showed that the nanosheets and TMDs consistently displayed surface ornamentation. Mo, S, and C were all discernible in the MoS_2@graphene EDAX image.

3.3. Raman Spectra Analysis

Figure 3 shows the results of Raman spectroscopy used to learn more about the films' architectural accuracy and the successful hybridization of graphene into MoS_2. The D and G bands of carbon are responsible for the Raman intensity peaks at 1356 cm^{-1} and 1553 cm^{-1} in pristine graphene [20]. The estimated ID/IG ratio is close to 1.28, suggesting that graphene was highly disordered. There are two Raman modes in the hexagonal structure of MoS_2 [21], designated E_{2g} at 375 cm^{-1} and A_{1g} at 411 cm^{-1}. NiS_2's pair libration vibration and phase stretching vibration are responsible for the peaks at 280 cm^{-1} and 490 cm^{-1} in Raman spectra [22]. The Raman spectra of NiS_2/graphene nanocrystals have been shown. Both the D band (with a peak at 1352 cm^{-1}) and the G band (with a peak at 1583 cm^{-1}) in graphene were found. I_D/I_G ratios of 1.05 for graphene and 1.32 for CoS_2/G indicate a significantly diminished sp2 carbon domain, respectively [23]. The I_D/I_G intensity ratio is enhanced [24], which may be due to CoS_2 intercalation into graphene causing the widely spread graphene layers.

3.4. DSSCs analysis

Sandwich-structure devices were constructed to test TMDs@graphene for their possible usage in DSSCs. Figure 4 depicts a schematic illustration of the final product. Photovoltaic metrics such as short circuit current density (Jsc), open circuit voltage (Voc), power conversion efficiency (PCE), and fill factor (FF) map to the J-V curves seen in Figure 5.

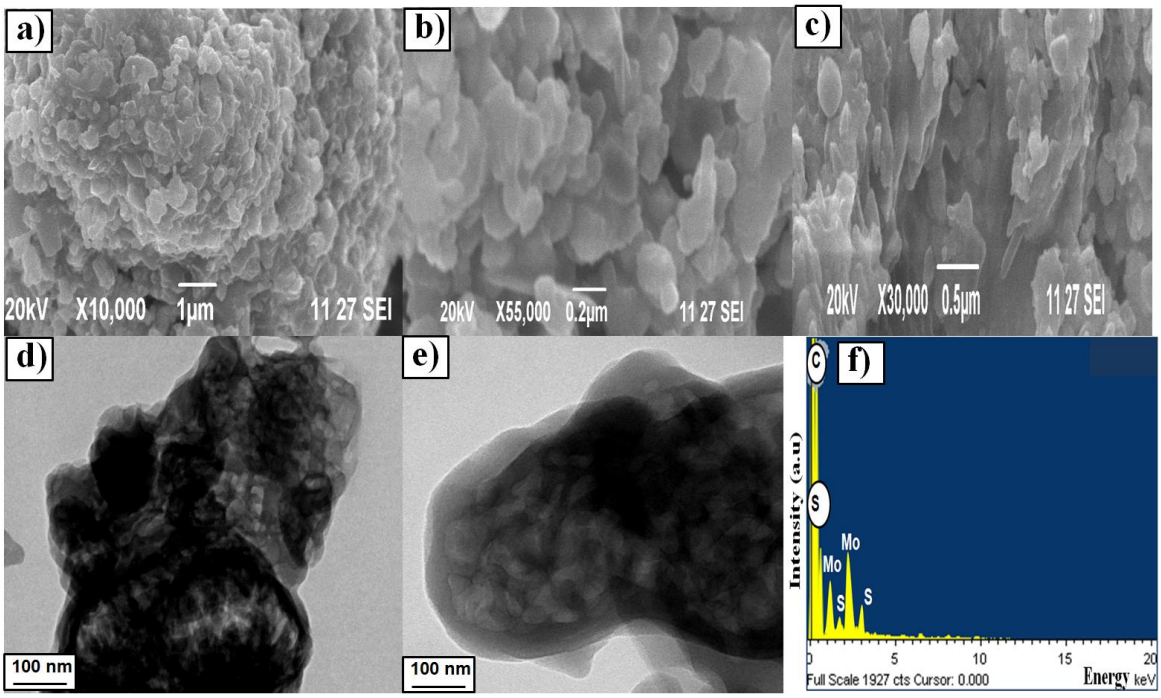

Figure 2. SEM images of **(a)** MoS_2@graphene; **(b)** NiS_2@graphene; **(c)** CoS_2@graphenel TEM images of **(d)** MoS_2@graphene; **(e)** NiS_2@graphene; EDAX image of **(f)** MoS_2@graphene

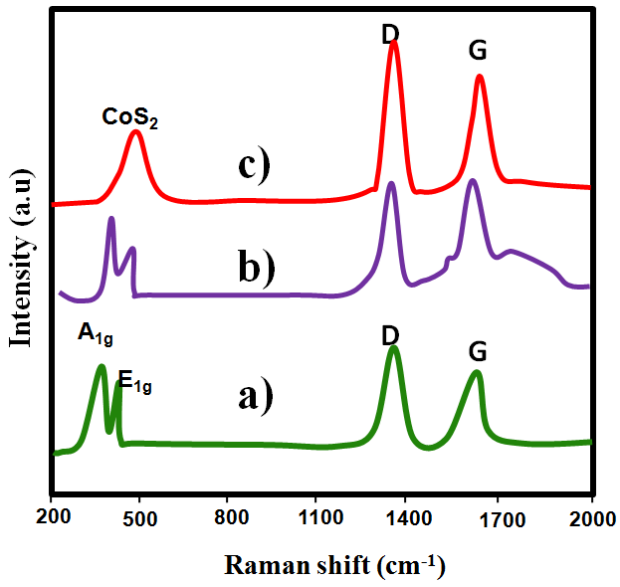

Figure 3. Raman spectra of **(a)** MoS_2@graphene; **(b)** NiS_2@graphene; **(c)** CoS_2@graphene

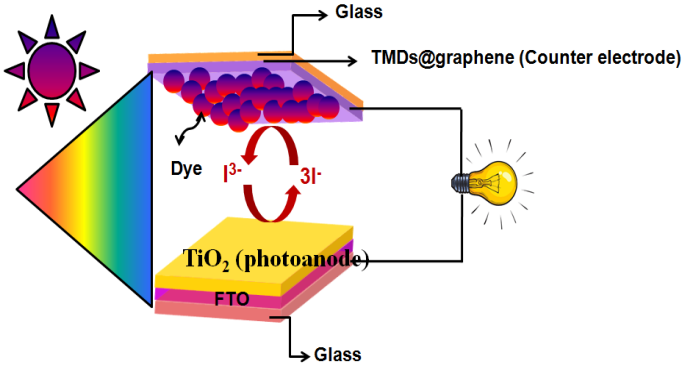

Figure 4. Schamatic representation of the fabricated DSSC

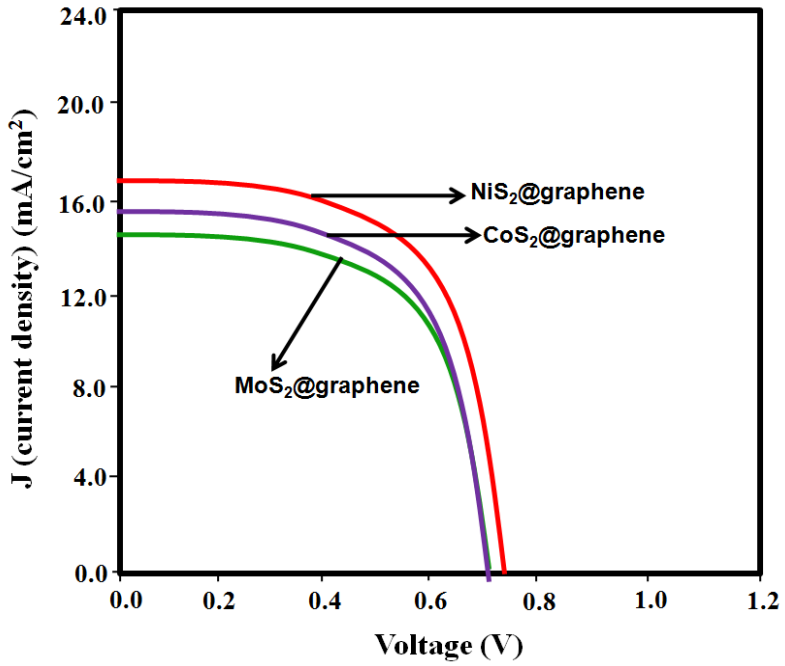

Figure 5. Current-voltage plot

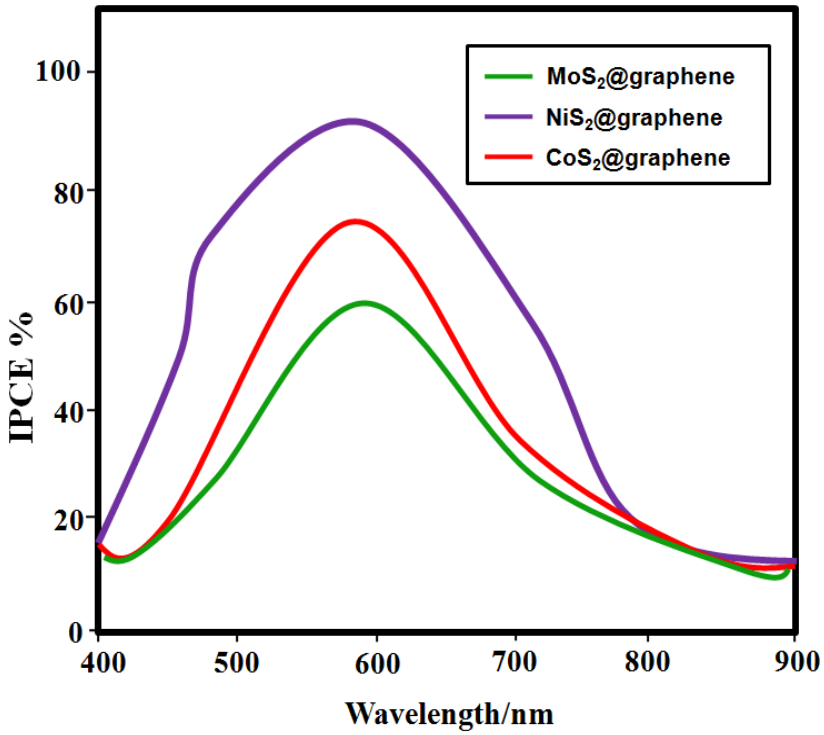

Figure 6. Incident photo-conversion electron plot

Table 1. Photovoltaic performance of DSSCs with various CEs under AM1.5G illumination (100 $mWcm^{-2}$)

CEs	V_{oc} (mV)	J_{sc} ($mAcm^{-2}$)	FF	PCE (%)
MoS_2@graphene	736	15.01	0.67	8.01 ± 0.05%
NiS_2@graphene	748	16.57	0.72	8.42 ± 0.05%
CoS_2@graphene	756	14.86	0.65	7.71 ± 0.03%

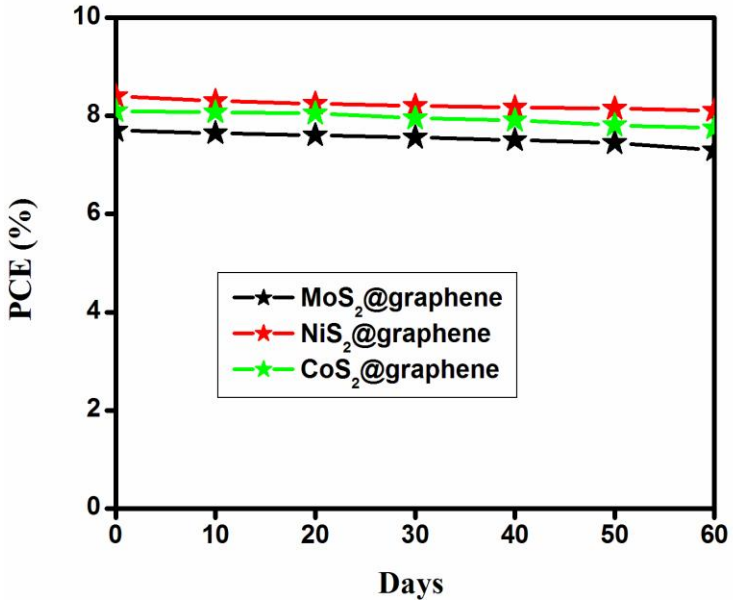

Figure 7. Long term stability plot of fabricated CEs

With a Voc of 748 mV, a Jsc of 16.57 $mAcm^{-2}$, and an FF of 0.72, the NiS_2@graphene CE DSSC achieved an overall PCE of 8.42±0.05%. The device utilizing NiS_2@graphene CE had a lower photovoltaic efficiency (Voc = 756 mV, Jsc = 14.86 mA cm^{-2}, FF = 0.65, = 7. 71± 0.03%) than the one without. Based on these comparisons, we may deduce that the enhancements to Jsc and FF are mostly responsible for the rise in PCE (Table 1). The improved Jsc may be linked back to the quick reduction of I_3^- ions by NiS_2@graphene, which in turn allows for faster regeneration of N719 molecules. These results were confirmed by the IPCE evaluation, which found that the NiS_2@graphene based device performed the best out of the three CEs under scrutiny (Figure 6). Similar trends were seen in the IPCE as were shown in the PCE and Jsc values, indicating that the as-prepared NiS_2@graphene CE was efficient in regenerating I_3^- ions in solution. We also conducted a long-term stability experiment lasting 60 days, checking the system every 10 days to ensure it was holding up. Under the same experimental parameters, the I-V characteristics of the device were measured, and the resultant graph is given in Figure 7. The PCE% has depreciated by just 1.85% after being tested for 60 days. The results show that the created device may be relied upon for lengthy periods of time and might have practical uses in photovoltaics.

4. Conclusion

Hydrid electrodes based on TMDs, such as MoS_2, NiS_2, and CoS_2, were successfully manufactured and used as counter electrodes in DSSC applications. The XRD results suggest that the manufactured samples are both very pure and nanocrystalline in nature. Scanning and transmission electron microscopy revealed an equal deposition of TMD nanoparticles on the graphene nanosheets' surface. Raman spectra showed that graphene had successfully hybridized with TMDs. The spectral analysis of the constructed sandwich DSSCs was investigated using J-V and IPCE measurements and comparisons. When compared to MoS_2@graphene (7.71± 0.03%) and CoS_2@graphene (8.01± 0.05%), the power conversion efficiency of the resulting NiS_2@graphene counter electrodes (CEs) was higher (8.42 ± 0.05%). The improved Jsc may be linked back to the quick reduction of I_3^- ions by NiS_2@graphene, which in turn allows for faster regeneration of N719 molecules. Because of this, these electrodes may serve as a suitable alternative to the platinum electrode often used in DSSC devices.

References

[1] A.S. Pawbake, M.S. Pawar, S.R. Jadkar, D.J. Late, Large area chemical vapor deposition of monolayer transition metal dichalcogenides and their temperature dependent Raman spectroscopy studies, Nanoscale, 8(5), (2016) 3008-3018. https://doi.org/10.1039/C5NR07401K

[2] A. Sinha, B. Tan, Y. Huang, H. Zhao, X. Dang, J. Chen, R. Jain, MoS2 nanostructures for electrochemical sensing of multidisciplinary targets: A review, TrACTrends in Analytical

Chemistry, 102, (2018) 75-90. https://doi.org/10.1016/j.trac.2018.01.008

[3] C. Yang, Y. Wang, Z. Wu, Z. Zhang, N. Hu, C. Peng, Three-dimensional MoS2/reduced graphene oxide nanosheets/graphene quantum dots hybrids for high-performance room-temperature NO2 gas sensors, Nanomaterials, 12(6), (2022) 901. https://doi.org/10.3390/nano12060901

[4] S. Kumar, D. Singh, D. Pathania, A. Awasthi, K. Singh, Molybdenum disulphide-nitrogen doped reduced graphene oxide heterostructure based electrochemical sensing of epinephrine, Materials Chemistry and Physics, 297, (2023) 127446. https://doi.org/10.1016/j.matchemphys.2023.127446

[5] S. Tajik, Z. Dourandish, F.G. Nejad, H. Beitollahi, P.M. Jahani, A. Di Bartolomeo, Transition metal dichalcogenides: Synthesis and use in the development of electrochemical sensors and biosensors, Biosensors and Bioelectronics, 216, (2022) 114674. https://doi.org/10.1016/j.bios.2022.114674

[6] J. Yang,L. Yang, X. Tang, Y. Zhang, Q. Dong, Z. He, N. Li, K. Huang, H. Luo, X. Xiong, ZIF derived N-CoS2@graphene rhombic dodecahedral nanocomposites: As a high sensitivity sensor for hydrazine, Sensors and Actuators B: Chemical, 351, (2022) 130967. https://doi.org/10.1016/j.snb.2021.130967

[7] S.Y.S. Jaberi, A. Ghaffarinejad, Z. Khajehsaeidi, A. Sadeghi, The synthesis, properties, and potential applications of CoS2 as a transition metal dichalcogenide (TMD), International Journal of Hydrogen Energy, 48(42), (2023) 15831-15878. https://doi.org/10.1016/j.ijhydene.2023.01.056

[8] B. Bor, B. Gogoi, B.M. Rajbongshi, A. Ramchiary, Nano-structured TiO2/ZnO nanocomposite for dye-sensitized solar cells application: A review, Renewable and Sustainable Energy Reviews, 81, (2018) 2264-2270. https://doi.org/10.1016/j.rser.2017.06.035

[9] T. Ma, J. Bai, C. Li, Facile synthesis of g-C3N4 wrapping on one-dimensional carbon fiber as a composite photocatalyst to degrade organic pollutants, Vacuum, 145, (2017) 47-54. https://doi.org/10.1016/j.vacuum.2017.08.027

[10] Y. Dong, L. Xing, F. Hu, A. Umar, X. Wu, Efficient removal of organic dyes molecules by grain-like α-Fe2O3 nanostructures under visible light irradiation, Vacuum, 150, (2018) 35-40. https://doi.org/10.1016/j.vacuum.2018.01.023

[11] P. Enciso, J.D. Decoppet, T. Moehl, M. Grätzel, M. Wörner, M.F. Cerdá, Influence of the adsorption of phycocyanin on the performance in DSS cells: and electrochemical and QCM evaluation, International Journal of Electrochemical Science, 11(5), (2016) 3604-3614. https://doi.org/10.1016/S1452-3981(23)17423-2

[12] M. Grätzel, Photo electrochemical cells, nature, 414(6861), (2001) 338-344. https://doi.org/10.1038/35104607

[13] Y. Li, H. Wang, H. Zhang, P. Liu, Y. Wang, W. Fang, H. Yang, Y. Li, H. Zhao, A {0001} faceted single crystal NiS nanosheet electrocatalyst for dye-sensitised solar cells: sulfur-vacancy induced electrocatalytic activity, Chemical communications, 50(42), (2014) 5569-5571. https://doi.org/10.1039/C4CC01691B

[14] X. Chen, Y. Hou, B. Zhang, X.H. Yang, H.G. Yang, Low-cost SnS x counter electrodes for dye-sensitized solar cells, Chemical Communications, 49(51), (2013) 5793-5795. https://doi.org/10.1039/C3CC42679C

[15] E. Bi, H. Chen, X. Yang, W. Peng, M. Grätzel, L. Han, A quasi core–shell nitrogen-doped graphene/cobalt sulfide conductive catalyst for highly efficient dye-sensitized solar cells, Energy & Environmental Science, 7(8), (2014) 2637-2641. https://doi.org/10.1039/C4EE01339E

[16] Y.L. Lee, C.L. Chen, L.W. Chong, C.H. Chen, Y.F. Liu, C.F. Chi, A platinum counter electrode with high electrochemical activity and high transparency for dye-sensitized solar cells, Electrochemistry Communications, 12(11), (2010) 1662-1665. https://doi.org/10.1016/j.elecom.2010.09.022

[17] Y. Li, W. Li, T. Ke, P. Zhang, X. Ren, L. Deng, Microwave-assisted synthesis of sulfur-doped graphene supported PdW nanoparticles as a high performance electrocatalyst for the oxygen reduction reaction, Electrochemistry

Communications, 69, (2016) 68-71. https://doi.org/10.1016/j.elecom.2016.06.006

[18] L. Deng, H. Fang, P. Zhang, A. Abdelkader, X. Ren, Y. Li, N. Xie, Nitrogen and sulfur dual-doped carbon microtubes with enhanced performances for oxygen reduction reaction, Journal of The Electrochemical Society, 163(5), (2016) H343. https://doi.org/10.1149/2.1131605jes

[19] Q.W. Jiang, G.R. Li, X.P. Gao, Highly ordered TiN nanotube arrays as counter electrodes for dye-sensitized solar cells, Chemical communications, (44), (2009) 6720-6722. https://doi.org/10.1039/B912776C

[20] J.S. Jang, D.J. Ham, E. Ramasamy, J. Lee, J.S. Lee, Platinum-free tungsten carbides as an efficient counter electrode for dye sensitized solar cells, Chemical Communications, 46(45), (2010) 8600-8602. https://doi.org/10.1039/C0CC02247K

[21] H. Sun, D. Qin, S. Huang, X. Guo, D. Li, Y. Luo, Q. Meng, Dye-sensitized solar cells with NiS counter electrodes electrodeposited by a potential reversal technique, Energy & Environmental Science, 4(8), (2011) 2630-2637. https://doi.org/10.1039/C0EE00791A

[22] M. Wu, X. Lin, A. Hagfeldt, T. Ma, A novel catalyst of WO2nanorod for the counter electrode of dye-sensitized solar cells. Chemical Communications, 47(15), (2011) 4535-4537. https://doi.org/10.1039/C1CC10638D

[23] F. Gong, H. Wang, X. Xu, G. Zhou, Z.S. Wang, In situ growth of Co0. 85Se and Ni0. 85Se on conductive substrates as high-performance counter electrodes for dye-sensitized solar cells. Journal of the American Chemical Society, 134(26), (2012) 10953-10958. https://doi.org/10.1021/ja303034w

[24] H. Geng, S.F. Kong, Y. Wang, NiS nanorod-assembled nanoflowers grown on graphene: morphology evolution and Li-ion storage applications. Journal of Materials Chemistry A, 2(36), (2014) 15152-15158. https://doi.org/10.1039/C4TA03440F

Does this article screened for similarity?

J. Dineshkumar: Conceptualization, Methodology, Validation, Investigation, Writing-Original Draft. R. Sakthivel: Formal Analysis, Investigation, Writing-Original Draft, Supervision. A. Geetha: Data Curation, Writing-Review & Editing. All the authors read and approved the final version of the manuscript.

Does this article screened for similarity?

Yes

Conflict of interest

The Authors declares that there is no conflict of interest anywhere.

About the License